(2)

STABLE INTEGRATED MICROWAVE TO OPTICAL MODULATOR

TECHNICAL/FINANCIAL REPORT - CDRL ITEM A001-7
(COVERING SEPTEMBER 2, 1991, TO DECEMBER 31, 1991)

PREPARED FOR:

OFFICE OF NAVAL RESEARCH
DEPARTMENT OF THE NAVY
ATTENTION: YP, CODE: 1212
CONTRACT NUMBER: N00014-90-C-0073
800 N. QUINCY STREET
ARLINGTON, VA 22217-5000

BY

WESTINGHOUSE DEFENSE AND ELECTRONICS CENTER
ADVANCED TECHNOLOGY DIVISION
P. O. BOX 1521
BALTIMORE, MD 21203

0322/jec

QUARTERLY REPORT FOR PERIOD 9/2/91 TO 12/31/91

1.0 Objective

The key technical objective for this research program is to integrate quantum well lasers (QWLs), detectors and GaAs MESFETs to produce a monolithic integrated microwave to optical modulator on semi-insulating GaAs substrates.

2.0 Programmatic Issues

Because of reduced funding levels, the work effort on this program was stopped effective 12/31/91. This final quarterly report covers the four month period from September 2, 1991, to December 31, 1991, the effective end of the program.

3.0 Technical Progress

3.1 University of Illinois

3.1.1 RIE Etching of Laser Facets

Reactive Ion Etching (RIE) was investigated in order to achieve vertical laser facets for integration purposes. Originally, we attempted to etch the GaAs/AlGaAs laser structures using plasmas from non-corrosive gases. A methane/hydrogen plasma was tried, but this resulted in an almost negligible etch rate for AlGaAs layers with mole fractions above 30% as well as formation of a hard-to-remove polymer due to the carbon and hydrogen in the plasma. An argon plasma was then tried due to its lack of selectivity in plasma etching. Unfortunately, etch rates greater than 90Å/min. could not be achieved.

At this point, it was evident that chlorinated plasmas must be used to obtain the etch rates necessary to isolate the laser cavities in a reasonable amount of time. Using $SiCl_4$, etches were performed on samples of GaAs and AlGaAs with mole fractions of 30, 50 and 60%. By varying the gas flow, pressure, and RF power, it was possible to etch the GaAs at rates of 6000 and 3350Å/min. At nearly the same parameters which the slower etch

rate was obtained, etch rates of 3100, 3200, 3400, and 3700Å/min. were obtained for AlGaAs samples with mole fractions of 0, 30, 50, and 60%, respectively.

Examination of these samples with the Scanning Electron Microscope (SEM) showed good vertical edge profiles (Figures 1-4). Also, immediately obvious are the tall pillar-like structures present on some of the samples (Figures 3 and 4). These undesirable items appear to be more numerous on samples with higher aluminum content and are believed to be due to oxidation of the surface of the GaAs samples during loading of the RIE. Etching of laser samples should not result in these structures because the AlGaAs layers are covered by a GaAs cap layer. Thus the AlGaAs layers are not exposed to oxygen at any time during the etch process.

Other plasma gases are also being explored for selective etching of the GaAs and AlGaAs layers which could be used for laser ridge formation.

3.1.2 High-Speed Laser Processing

Three laser structures were grown on semi-insulating GaAs substrates: two by MOCVD and one by MBE. The first MOCVD structure was a standard Single-Quantum-Well Separate-Confinement-Heterostructure (SQW-SCH) with no graded layer compositions, i.e., no GRIN layers. This is a structure that our MOCVD crystal growers have produced many times on n+ GaAs substrates, producing laser devices that typically demonstrate very low threshold current densities (typically as low as 150Å/cm^2). The second MOCVD wafer was similar to the first, the only exception being that the quantum well was repeated three times, yielding a Multi-Quantum-Well (MQW-SCH) structure. As predicted by theory, we expected the MQW devices to demonstrate higher intrinsic response speeds than the SQW devices, along with somewhat higher threshold current densities. The single MBE structure was a MQW-GRINSCH structure (three quantum wells with parabolic-graded refractive index transitions from cladding to active layer). This structure

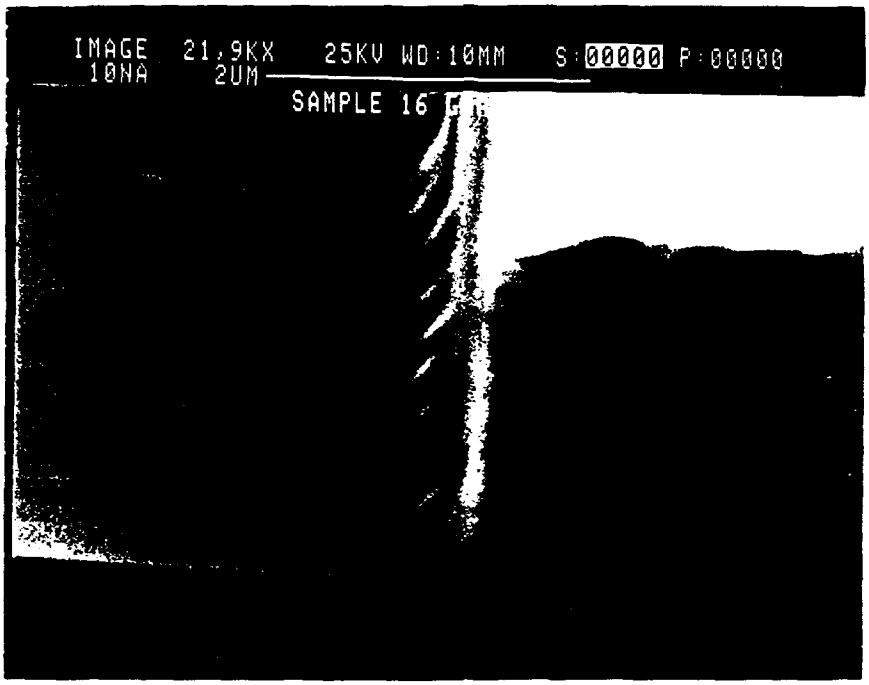

Figure 1. SEM Photograph of RIE Etched Ridge GaAs.

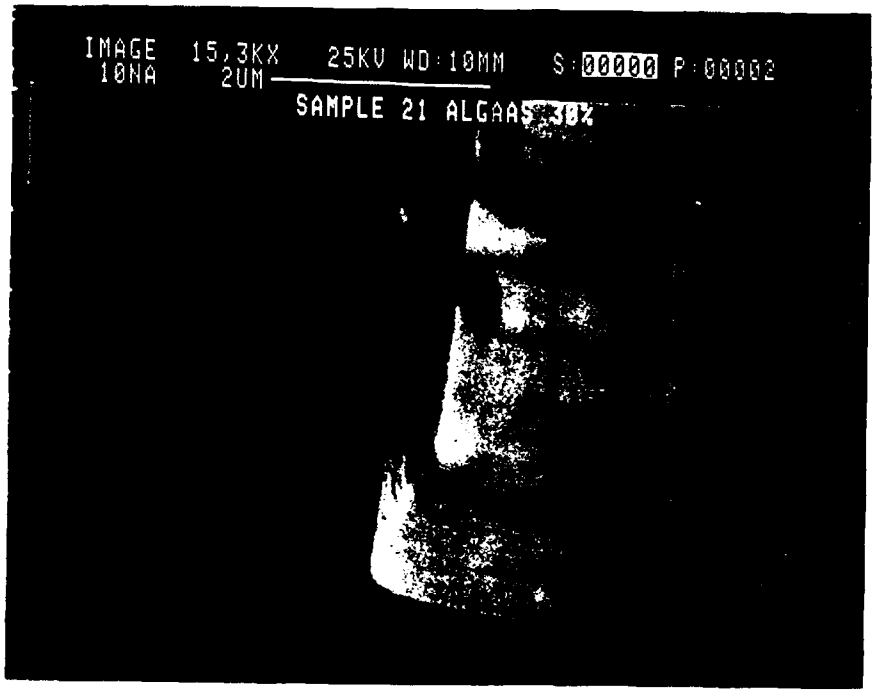

Figure 2. SEM Photograph of RIE Etched Ridge in AlGaAs (30% Al).

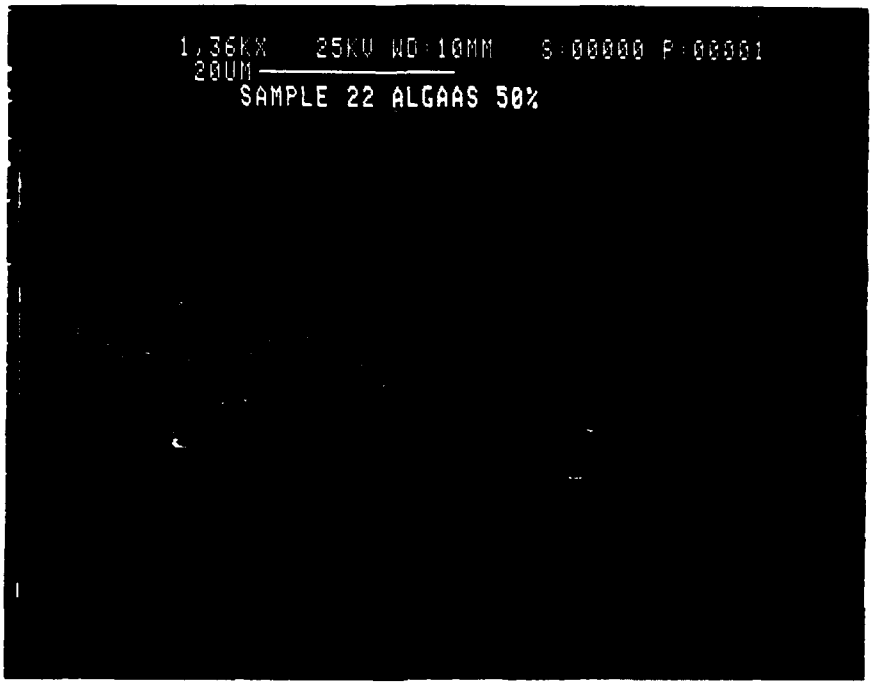

Figure 3. SEM Photograph of RIE Etched Ridge in AlGaAs (50% Al).

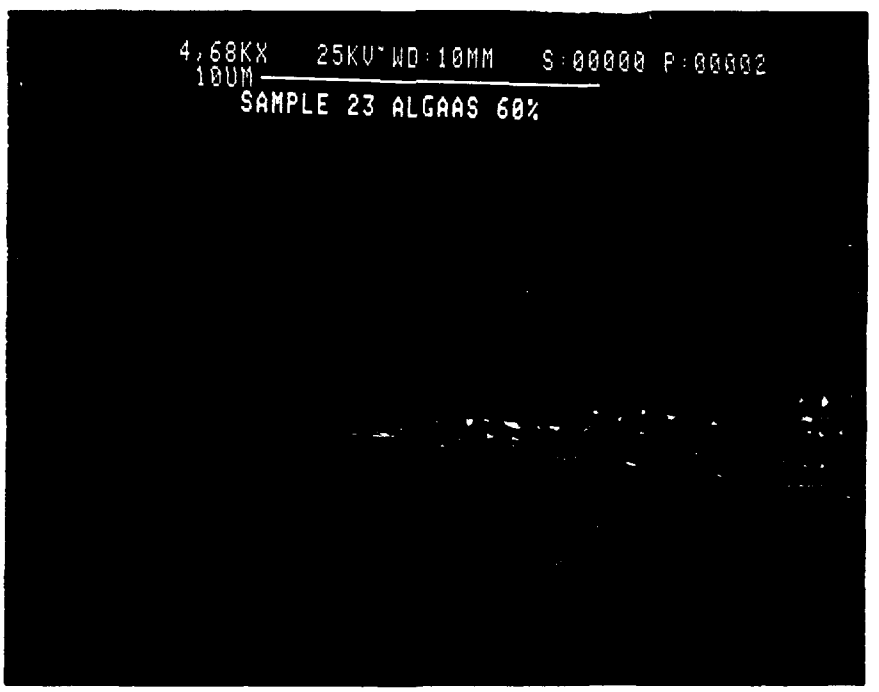

Figure 4. SEM Photograph of RIE Etched Ridge in AlGaAs (60% Al).

was expected to demonstrate improved performance over the MOCVD-grown MQW-SCH (no graded layer compositions) particularly in terms of response speed.

The two MOCVD structures were first fabricated into large-area devices. Threshold current densities were measured and found to be favorably low (approximately 400Å/cm^2) for the MQW devices. The SQW devices, however, demonstrated thresholds three times higher than identical structures fabricated on n+ substrates. This is due to too thin n-type contacting layers within the structures, as well as possible defect propagation from the semi-insulating substrates.

Next, both the MOCVD and MBE wafers were fabricated into ridge-waveguide devices for high-frequency operation and testing. These devices are designed for electrical contacting through Cascade Probes (see Figure 5). The probes are constructed such that a high-frequency 50 ohm transmission line (bandwidth in excess of 30 GHz) is brought directly to the probe tips. Thus, this probing scheme allows us to send and receive high-frequency signals without wire-bonding or other contacting schemes, making it possible for a large number of high-frequency devices to be characterized without expensive and time-consuming high-frequency packaging. In addition, these devices are particularly well suited for integration, as the contacts can be coplanar.

Currently we are testing these devices both for threshold current values and speed of response. For the speed measurements we are using an HP 8620C Sweep Oscillator with plug-in units capable of delivering signals from 10 MHz up to 18.6 GHz. In addition, the light output of the laser is being measured by a New Focus GaAs detector with 45 GHz bandwidth. We expect the bandwidth of the MQW devices to exceed that of the SQW devices, as predicted by theory, however, we do not have a clear estimate for what the absolute values of modulation bandwidth will be.

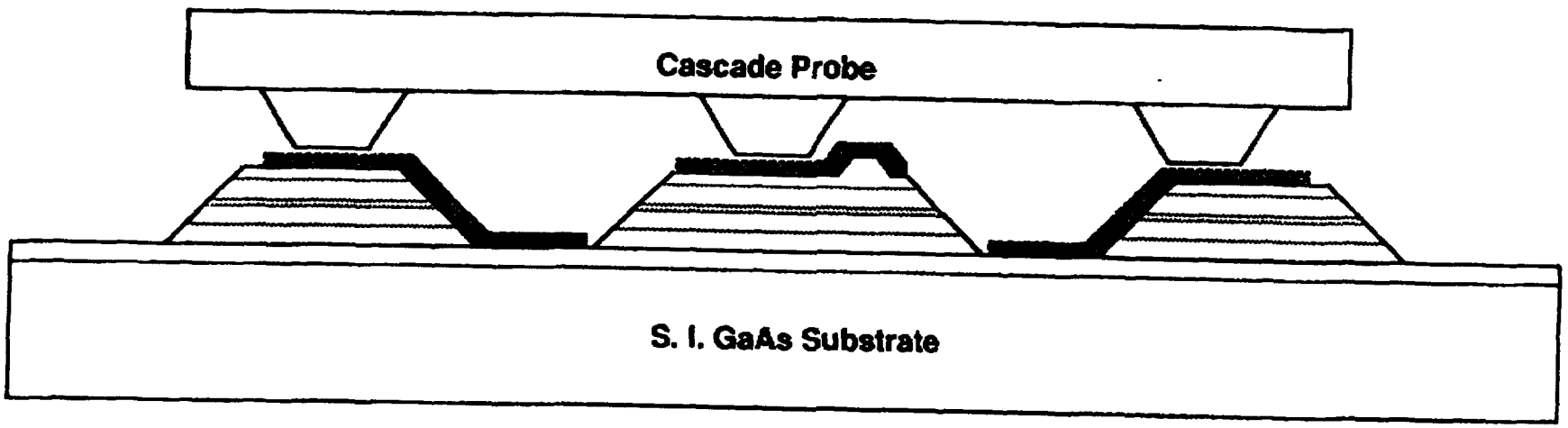

Figure 5. Cascade Probeable Ridge-Waveguide Laser

3.2 Westinghouse

3.2.1 Stabilization Loop

In the current reporting period good progress has been made in the development of stabilization loop circuitry, following up on work undertaken in the previous quarter. Referring to the report for that period, it was indicated that the gain of a constant current amplifier stage was limited to approximately X13 because of trade-offs associated with MESFET doping profile in use. The gain stage was nevertheless embedded in the stabilization loop, achieving a figure of merit of $\geq$ 50 with 70 mA of laser diode current and optical coupling between laser and photodiode adjusted to yield a 16 microamp photodiode current. Figure of merit, as a measure of loop gain, will be discussed later in this report in conjunction with the measuring technique shown in Figure 8.

Open loop gain for the system under discussion may be expressed as:

$$G_o = J_C * R_{LPD} * G_P * g_{fs} * E_{SL} \qquad \text{(Equation 1)}$$

where: J_C = Coupled responsivity of the loop monitor photodiode (amps/watt)

R_{LPD} = Value of photodiode load resistor (ohms)

G_P = Gain of photodiode pre-amp stage

g_{fs} = Forward transconductance of source follower stage at laser operating current (Siemens)

E_{SL} = Low frequency slope efficiency of laser diode (watts/amp) (For HLP-1400 typ. 0.13 w/a)

The HLP-1400 laser diode typically produces 6 mW output at a 70 mA operating point indicating a coupled responsivity of 2.7×10^{-3} when coupling is adjusted for a 16 microamp photodiode current. If we take the following representative values of R_{LPD} = 91 x 10^3 ohm, G_P = 12, g_{fs} = .09 S, and E_{SL} = 0.3 watts/amp, then G_o = 80 which is comfortably in excess of the measured figure of merit values in the range of 50 to 60. These measured values were approximately halved as expected when optical coupling was

reduced to yield photodiode currents in the target range of 8-10 microamps, ($\eta_c = 1.4 \times 10^{-3}$ amps/watt).

It should be noted that the target photocurrent applies for laser diode currents in the vicinity of the selected operating point of 70 mA. Selection of other operating points in the linear region above laser threshold will yield other values of photocurrent with little impact on loop gain, whereas changes in photocurrent resulting from changes in optical coupling will directly impact η_c and thus loop gain. Equation 1 also indicates that to achieve the goal of a figure of merit of 100 with $\eta_c = 1.43 \times 10^{-3}$, the pre-amp stage gain G_P needs to be increased to approximately X40 for a calculated $G_o = 138$.

The shunted cascode gain stage proposed earlier lends itself to modifications which enhance the gain, the revised configuration being shown in Figure 6. Here the application of ± 7 volt power supply rails has allowed the use of higher R_L and R_{SH} values, and Q_2 gate is biased from a Photovoltaic Isolator operating from the -7 V rail which eliminates the need for level shifting diode(s) in the Q_2 source. A current limiting resistor in the drain of Q_3 has been added to protect the laser diode from potentially damaging current spikes. The shunted cascode stage achieved a measured low frequency gain of X40, indicating a Q_2 operating g_{fs} of > .02 S at a drain current of 14 mA. The gain enhancement relative to the constant current design is primarily due to the higher operating g_{fs} of Q_2 which both reduces the shunting effect of g_{os} on R_L and contributes directly to the gain term $-g_{fs}R_L$. As in the case of the constant current design it has been necessary to apply ferrite absorbing material to the drain leads of Q_2 to suppress the tendency for microwave oscillation. It is anticipated that circuit integration as shown in Figure 7 will drastically reduce lead inductances and obviate this tendency.

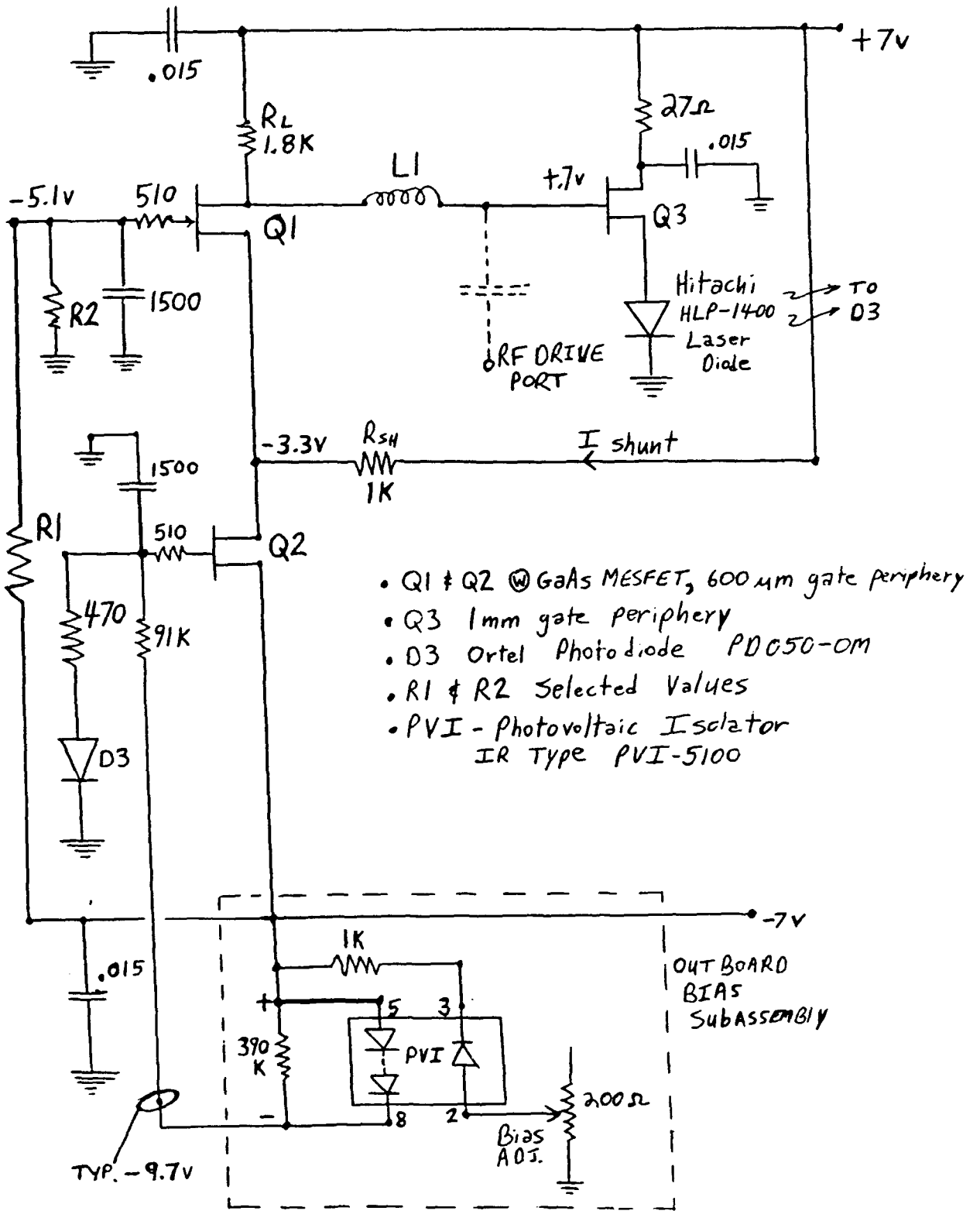

Figure 6. Stabilization Loop Using Shunted Cascode Gain Stage.

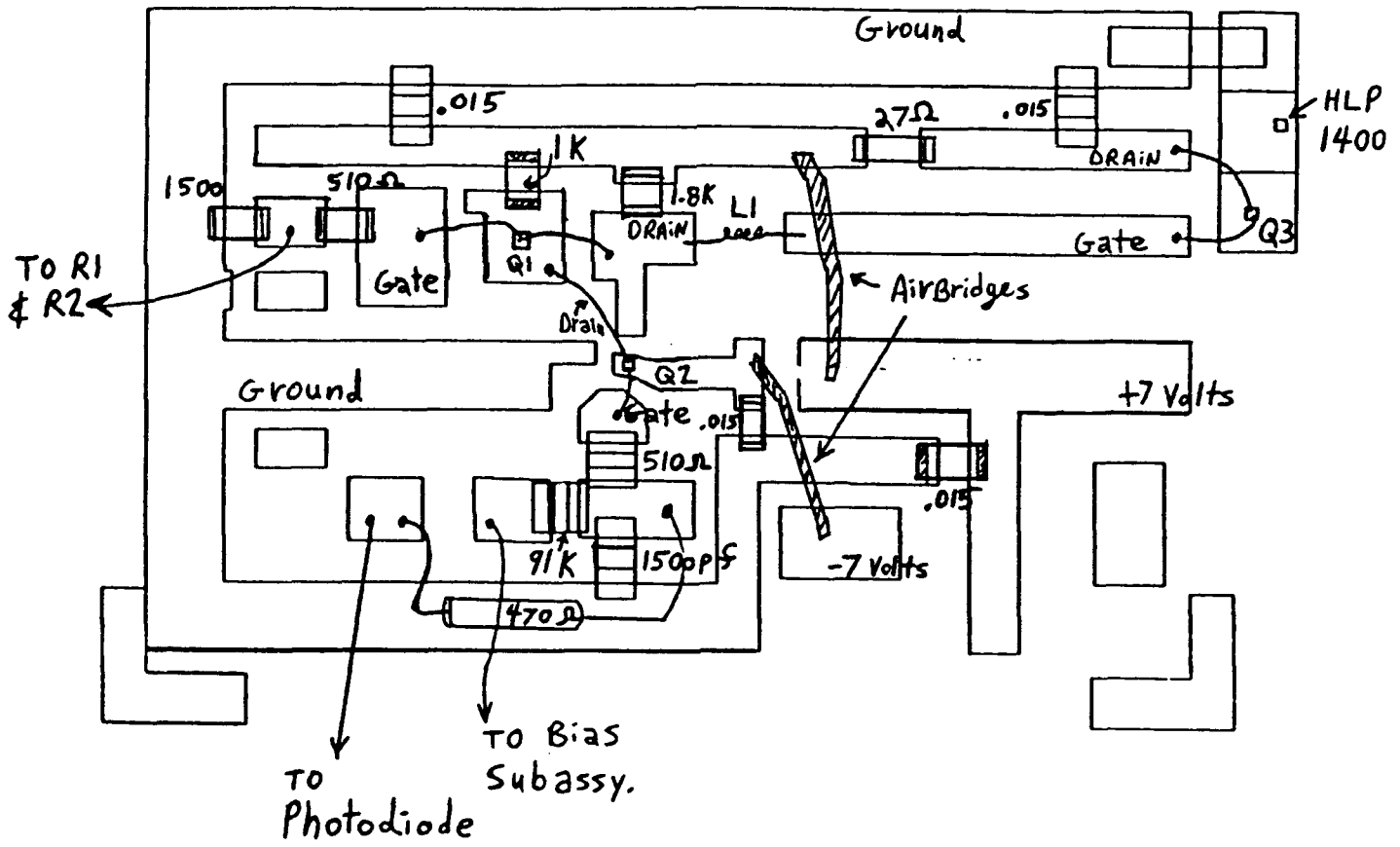

Figure 7. Substrate Layout for Stabilization Circuit.

It was concluded that the shunted cascode design will be able to satisfy the closed loop figure of merit goal, but complete experimental verification will require laser diode/photodiode samples from the University of Illinois. Provisional verification using the configuration shown in Figure 8 is currently in progress and will be completed when a new HLP-1400 laser diode (on order) is received. The figure shows the use of previously described coupling optics to couple laser and photodiode with displacement of the photodiode with respect to the output focus as coupling adjustment. A beam splitter in the collimated space extracts an 8% beam sample unaffected by coupling adjustment and this is detected by a large area photodiode, any modulation on the laser diode output being amplified and presented on the scope display. A figure of merit measurement is made by comparison of scope display amplitudes under open and closed loop conditions with a small excursion perturbation current fed into the photodiode load resistor (R_{PD}) from a constant current source. Under open loop conditions (S_1 open) the constant current 10 Hz stimulus in R_{PD} produces an EMF which modulates the laser and is detected by the large area photodiode and displayed and measured on the scope. With S_1 closed the modulated photocurrent in R_{PD} produces an EMF across it which is anti-phase to that induced by the constant current stimulus. This results in a much reduced laser depth of modulation for a given 10 Hz stimulus, and a correspondingly reduced amplitude of scope display. The ratio of open to closed loop scope deflections is thus a measure of "figure of merit" and a useful indicator of loop stiffness in the presence of system perturbations. During all measurements, laser diode current is maintained at the selected operating point for closed loop operation (70 mA) by adjustment of the negative bias applied to R_{PD}. Although the bias voltages differ by a fraction of a volt under open and closed loop conditions, the small change in reverse bias on the

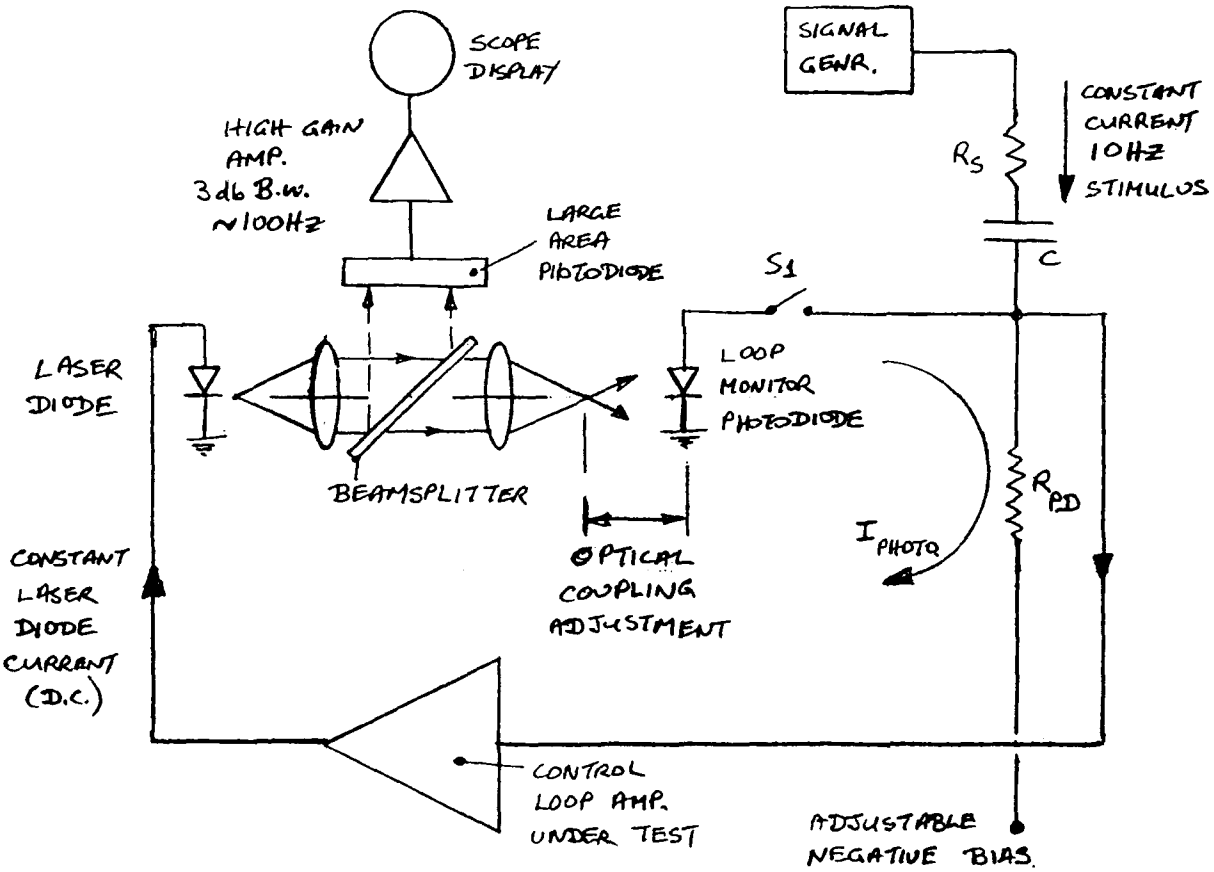

R_{PD} – PHOTODIODE LOAD

R_S – CONSTANT CURRENT SOURCE

C – D.C. BLOCKING

Figure 8. Figure of Merit Measurement.

photodetector has a negligible effect on coupled responsivity J_c.

In the next quarter we had planned to proceed with the circuit integration process and to complete the provisional figure of merit measurements using a new HPL-1400 laser diode. However, because of the funding situation, this effort has been stopped effective December 31, 1991.

4.0 Financial

Program spending to December 31, 1991, both planned and actual, is shown in Figure 9. The figures shown are direct cost and do not include G&A or Fee. Program spending has been stopped except for closeout activities. November and December, 1991, invoices from the University of Illinois will be paid early in 1992 completing program spending.

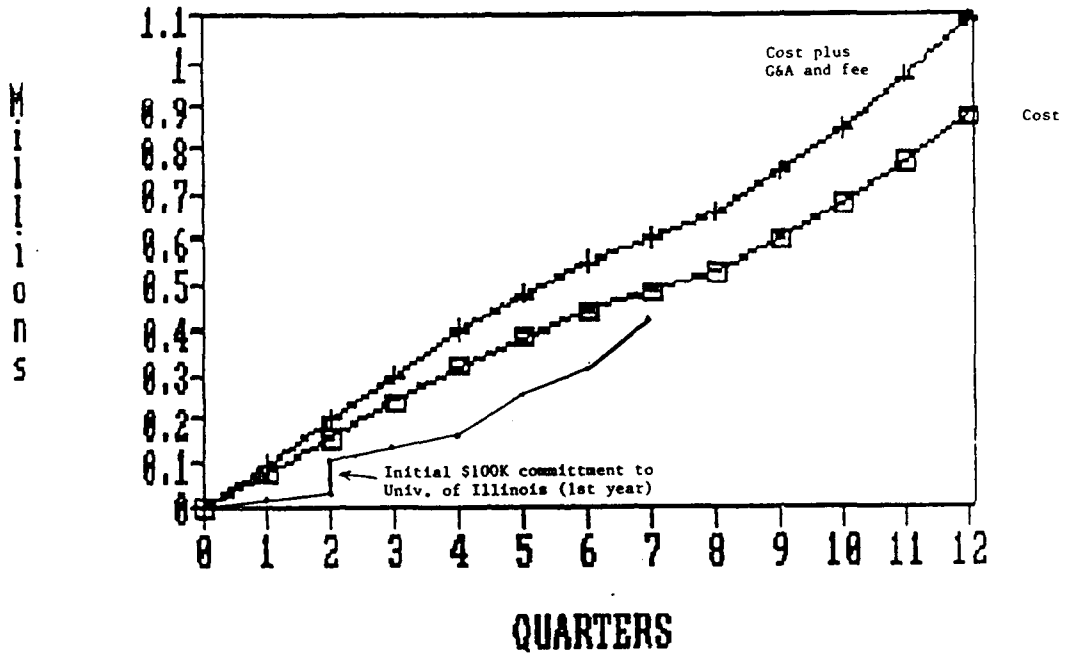

Figure 9. Program Spending.

James E. Degenford
Program Manager